1-7-1997

Progress in the study of CdZnTe strip detectors

O Tousignant
University of Montreal

L A. Hamel
University of Montreal

J F. Courville
University of Montreal

P Paki
University of Montreal

John R. Macri
University of New Hampshire - Main Campus, John.Macri@unh.edu

See next page for additional authors

Recommended Citation

Olivier Tousignant ; Louis-Andre Hamel ; Jean-Francois Courville ; P. Paki ; John R. Macri ; Kipp Larson ; Michelle Mayer ; Mark L. McConnell and James M. Ryan "Progress in the study of CdZnTe strip detectors", Proc. SPIE 3115, Hard X-Ray and Gamma-Ray Detector Physics, Optics, and Applications, 214 (July 7, 1997); doi:10.1117/12.277688; http://dx.doi.org/10.1117/12.277688

Progress in the study of CdZnTe strip detectors

O. Tousignant, L.A. Hamel, J.F. Courville, P. Paki

Groupe de recherche en physique et technologie des couches minces (GCM),

University of Montreal,

Montreal, H3C 3J7, Canada

J.R. Macri, K. Larson, M. Mayer, M.L. McConnell, J.M. Ryan

Space Science Center,

University of New Hampshire

Durham, NH 03824, USA.

ABSTRACT

We report new performance measurements and computer simulations of a sub-millimeter pitch CdZnTe strip detector under study as a prototype imaging spectrometer for astronomical X-ray and γ-ray observations. The prototype is 1.5 mm thick with 375 micron strip pitch in both the x and y dimensions. Previously reported work included demonstrations of half-pitch spatial resolution ($\sim$ 190 microns) and good energy resolution and spectral uniformity. Strip detector efficiency measurements have also been presented. A model that includes the photon interaction, carrier transport and the electronics was developed that qualitatively reproduced the measurements.

The new studies include measurements of the CdZnTe transport properties for this prototype in an effort to resolve quantitative discrepancies between the measurements and the simulations. Measurements of charge signals produced by laser pulses and α-rays are used to determine these transport properties. These are then used in the model to predict γ-ray efficiencies that are compared with the data. The imaging performance of the detector is studied by scanned laser and gamma beam spot measurements. The results support the model's prediction of nearly linear sharing of the charge for interactions occurring in the region between electrodes. The potential for strip detectors with spatial resolution much finer than the strip pitch is demonstrated. A new design scheme for strip detectors is shortly discussed.

Keywords: CdZnTe, strip detector, charge transport, signal generation, simulation, modeling, imaging, X-ray, gamma-ray

1. INTRODUCTION

Sub-millimeter resolution CdZnTe position-sensitive detector technology offers a promising prospect for achieving both improved energy and spatial resolution with high stopping power without the need for cryogenic cooling.[1–7] An apparent advantage of CdZnTe strip detectors employing orthogonal anode and cathode strips is that they define an N x N pixel imaging area with only 2N signal processing channels.[1] Good energy resolution, spectral uniformity and sub-millimeter spatial resolution have been demonstrated with CdZnTe strip detectors.[1,2,4,6,7] A spatial resolution of less than 50 μm has been demonstrated at 22 keV with 100 μm pitch strip detectors.[6] Strip detectors, however, must rely on efficient transport of both electrons and holes for coincident anode and cathode signal measurement. The poor and widely varying hole transport properties[1,2,7,12,15] of currently available materials result in non-uniform response to photons interacting at different regions of the detector.[2] This must be considered when designing strip detector systems for specific applications.

An appropriate model for the charge transport and signal generation processes in CdZnTe detectors is an essential tool for understanding the detector performance characteristics and can be used to help specify optimum detector

Further author information: O.T. (correspondence)
O.T.: Email: tousi@lps.umontreal.ca; Telephone: (514) 343-6204; Fax: (514) 343-6215
J.R.M.: Email: John.Macri@unh.edu; Telephone: (603) 862-2793; Fax: (603) 862-4685.

SPIE Vol. 3115 • 0277-786X/97/$10.00

geometries and signal processing electronics for each application.[7–11] Use of such a model will help minimize the number of expensive and time consuming hardware prototypes required in any development effort. Achieving agreement between simulations and strip detector prototype measurements will be a significant developmental milestone and is a major goal of our present work.

2. SIMULATION MODEL

Our model is intended to be an end-to-end tool for simulating all detection and measurement processes from the radiation interaction down to the electronic chain. The detector material (mobilities, trapping and detrapping coefficients), bias and geometry (thickness, electrode pitch and gap) of the detector are incorporated in the model. In the case of γ-rays, a GEANT module first simulates photon interactions to provide initial electron-hole pair distributions that vary from event to event. For alphas and laser pulses, the pair generation is considered to occur essentially at the surface of incidence, i.e. either at the anode (z=0) or the cathode ($z = L$) plane, where L is the detector thickness.

A charge transport and signal generation module then computes the signal induced on any electrode by carriers drifting in the detector. The transport part of the simulation consists of an analytical solution of the continuity equations that provides the free electron and hole densities $n_e(x,t)$ and $n_h(x,t)$ in the detector in the presence of trapping and detrapping.[11]

The current through a given electrode j is obtained by integrating $en(\vec{x},t)\mu\vec{F}(\vec{x}) \cdot \vec{F}_{wj}(\vec{x})$ throughout the detector volume, where $\vec{F}(\vec{x})$ is the electric field in the detector and $\vec{F}_{wj}(\vec{x})$ is the weighting field for the given electrode j.[2,7,10] The weighting potential $\vec{\Phi}_{wj}(\vec{x})$ is obtained by solving the Laplace equation in the detector with appropriate boundary conditions.[2] Figure 1 (left) shows the weighting potential map for the cathode strip j as a function of x, the lateral position perpendicular to the cathodes, and z, the depth in the detector, measured from the anode plane. Since the anode and cathode strips are identical in width and pitch, the weighting potential for anodes is identical but for obvious coordinate changes. Figure 1 (right) shows the longitudinal (z) component of the weighting field along the axis of the electrode j under consideration and along the axis of its immediate neighbors $j \pm 1$.

The increased weighting field close to the electrode j is clear and leads to the position sensitivity of the electrode and to an improved energy resolution for anodes (compared to cathodes) since they are less sensitive to holes drifting in the opposite direction. The bipolar shape of the weighting field on neighboring electrodes will produce small transient signals though no net charge may be collected.

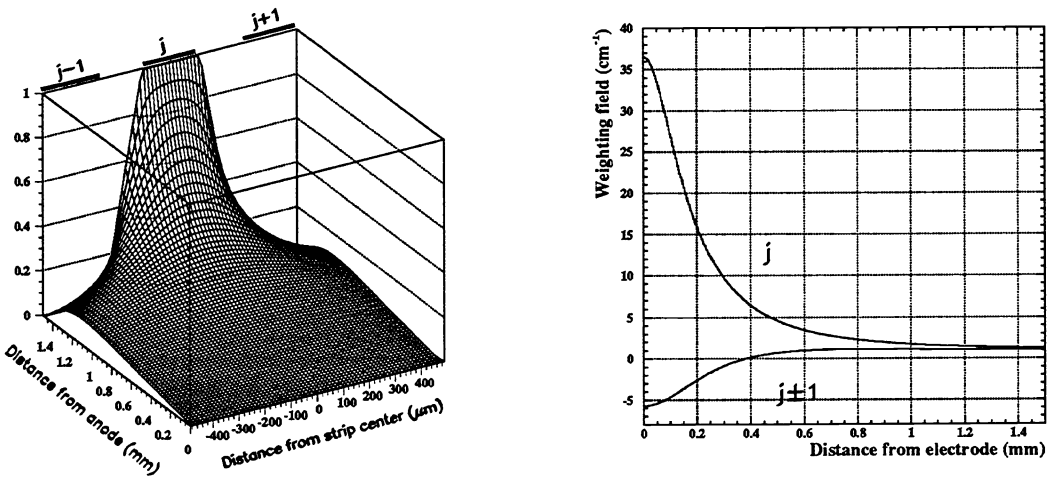

Figure 1. Left: The cathode weighting potential. Right: The weighting field as a function of the distance from an electrode along an axis centered on the electrode j and along an axis centered on its neighbor $j\pm1$.

3. CHARGE TRANSPORT PROPERTIES

3.1. Measurement setup

Figure 2 represents a small segment of the prototype $Cd_{0.9}Zn_{0.1}Te$ strip detector, the electrode geometry, the coordinate system and the electronics used for these measurements. Illumination from the cathode side by the scanable focused pulsed laser beam is also illustrated. Orthogonal anode and cathode strips have the same geometry: strip pitch is 375 μm, with 225 μm wide gold contact strips and 150 μm gaps (spaces) between the electrodes. Although not shown, all strips on each surface are biased via 1GΩ load resistors and untested strips are ac coupled to ground. Charge sensitive preamplifiers (eV-5093) process the ac coupled signals from four contiguous strips on each surface. Simultaneous signals are recorded for subsequent analysis on two 4-channel digital oscilloscopes (Tektronix, models 460 and 420). The cathodes X-strips (top side) are at ground potential. The typical bias, applied to the anodes, Y-strips (bottom side), was +200 V. This bias voltage and polarity was used for all reported measurements unless noted otherwise. Illumination with the laser was always from the top (X-strip) side. Illumination with α-, X- and γ-rays was possible from either side.

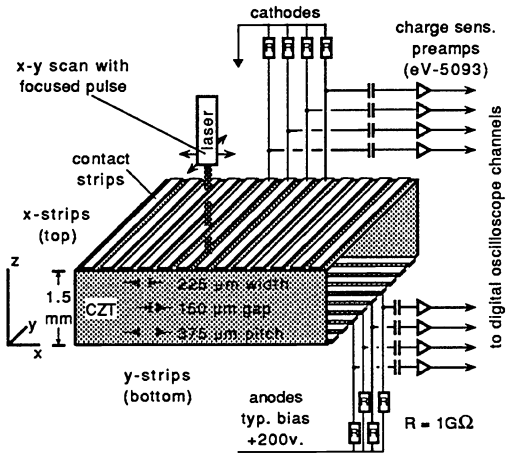

Figure 2. Small segment of the prototype strip detector.

3.2. Laser-induced signals

The laser used for these measurements is a nitrogen-pumped dye laser operating at a wavelength of approximately 500 nm (green light) and providing short (<5 ns) pulses. The absorption length at 500 nm in CdZnTe is much less than a micron and electron-hole pairs may be considered to be generated at the surface. Transient charge signals induced on various electrodes following short laser pulses were recorded in order to study the charge transport characteristics of the prototype CdZnTe strip detector. In this series of measurements, the detector was scanned in fine steps in the x and y directions by a collimated laser beam of approximately 40 μm in diameter. Signals from the charge preamplifiers were simultaneously recorded for all strips showing a sizable signal. Figure 3 a) shows signals on three contiguous anodes and three contiguous cathodes that are induced by the transit of electrons following one laser pulse incident on the cathode plane in the middle of the intersection region defined by cathode X16 and anode Y6. Figure 3 b) shows the signals on the same electrodes for the laser beam incident in the gap, i.e. at the midpoint between cathodes X15 and X16 and anodes Y5 and Y6. The signals are positive on the anodes and negative on the cathodes because they are inverted by the preamplifiers.

With the laser aimed in the center of an anode (cathode), large signals are induced only on the addressed anode (cathode). When illuminating the center of the gap, the signal is equally shared between the two neighboring anodes (cathodes). A short delay is observed between cathode and anode signals of the order of the transit time. The electrons first induce a large positive current in the cathode when they start receding from it, the current quickly decreasing when electrons move in the region of lower weighting field (see fig. 1 right). On the other hand, the anode current is small at the beginning and increases to its maximum near the end of the transit when electrons get closer to the anode.

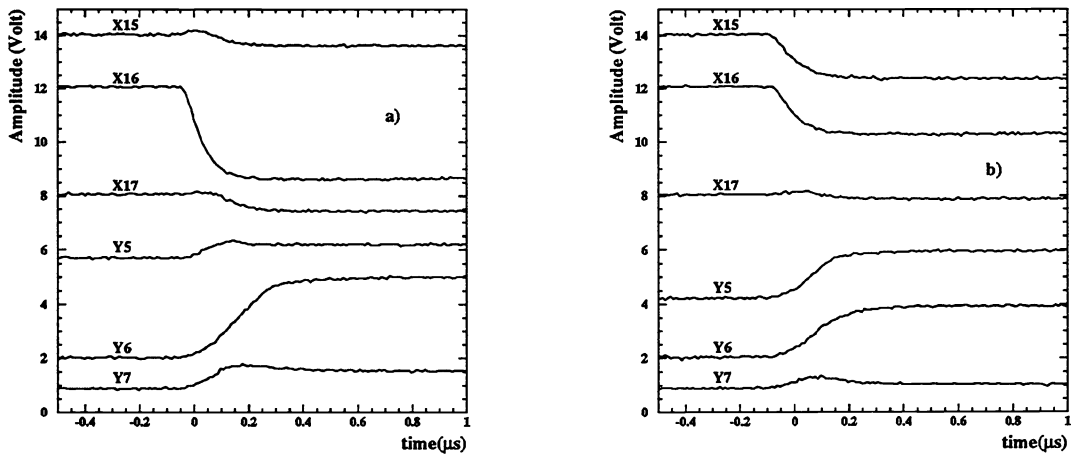

Figure 3. Electron charge signals on three contiguous anodes and three contiguous cathodes with a) the laser centered on cathode X16 and anode Y6 and b) the laser in the center of the gap between cathodes X15 and X16 and between anodes Y5 and Y6.

Smaller signals are also measured on other nearby electrodes. These signals show two components. A transient signal is induced by electrons drifting from the point of interaction down to the collecting anode, producing a positive lobe (after inversion by the preamplifier) that should return to zero after the transit time, on electrodes on which no net charge is collected. But these small signals clearly show some net residual charge after the transit time. This indicates that either lateral diffusion takes place or that the laser spot is larger than the strip width of 225 μm. But the laser beam profile was measured and showed negligible intensity beyond a radius of 50 μm. Also, the residual charge on the side electrodes is smaller on the cathodes than on the anodes. These observations clearly favor diffusion. Though small, the charge spreading remains larger than expected by normal diffusion.

Hole signals produced by the laser pulses (not shown) were also recorded by inverting the detector polarity. The induced charge on all collecting electrodes was then much smaller than for electrons indicating the well known fact that holes are strongly trapped in CdZnTe.

These observations suggest that space charge effects might influence carrier movement. Given the preamplifier sensitivity, the electron signals shown on figure 3 correspond to 1.4 pC or 40 MeV in CdZnTe, the energy deposition occurring in a very thin layer. Plasma effects might then delay the charge separation and produce lateral diffusion. Indeed risetimes of laser induced signals are somewhat longer than expected. In order to understand this effect, signals produced by 5.5 MeV α-rays were also recorded and are discussed in the next section.

3.3. Signals induced by alphas

Several signals on neighboring anodes Y5 and Y6 were simultaneously recorded with the oscilloscope triggered on Y6. Figure 4 (left) shows one event for which the interaction occurred directly on the strip Y6. Similarly, figure 4 (right) shows cathode signals on X15 and X16 for an event occurring immediately on X16. In both cases, a large signal is measured on the main electrode while no net charge is collected on its neighbors. The fact that no charge is collected on Y5 and Y7 (not shown) shows that electrons suffer no measurable diffusion during their transit to the anode plane. The risetimes are also shorter for these alpha signals than for the laser signals. This demonstrates that a component of the signal observed during the laser experiment was indeed produced by space charge effects. The laser setup will be optimized to allow measurements with less intense laser pulses.

In addition to the measured signals, figure 4 also shows the result of our simulations for an alpha interacting at the cathode plane in the center of anode Y6 and cathode X16. An excellent agreement is obtained with the transport parameters of table 1. Note that the simulated signals also include an effective integration time of 20 ns to account for the electronics risetime. This limited risetime being not much shorter than the features in the measured signals, these trapping and detrapping constants may not be very accurate. Nevertheless, the agreement with the model is satisfactory, at least on the time scale of interest for radiation detection. These parameters yield an effective electron drift mobility, $\mu_{\text{eff}} = \mu\tau_t/(\tau_t + \tau_d)$ of about 660 $\text{cm}^2\text{V}^{-1}\text{s}^{-1}$, where τ_t and τ_d are the trapping and detrapping times respectively.

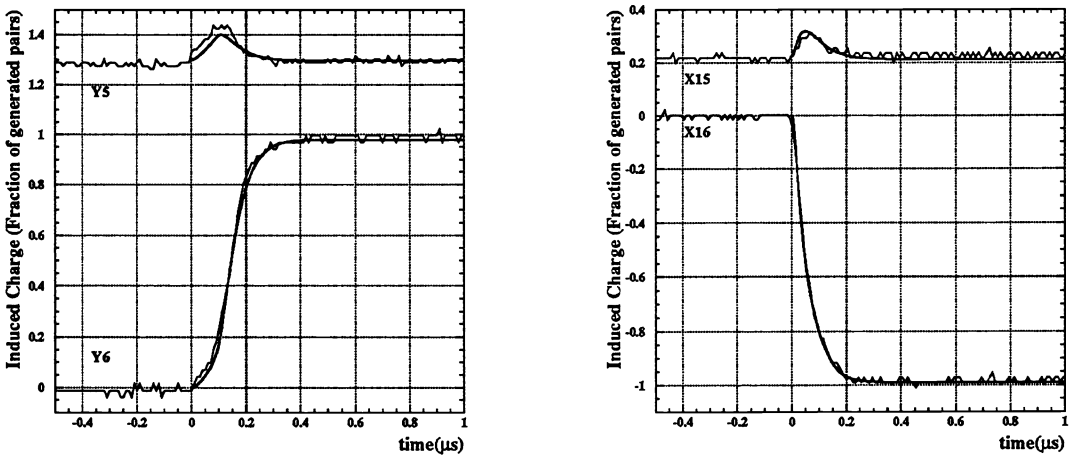

Figure 4. Measured and simulated electron signals on two neighboring anodes (Y5 and Y6) and cathodes (X15 and X16) due to alphas incident on the cathode plane in the center of anode Y6 (left) and in the center of cathode X16 (right).

Hole transit signals produced by alphas were also measured. Figure 5 shows such a cathode signal for the alpha interacting in its center. It is much smaller than corresponding electron signals, indicating that most holes were trapped before reaching the cathode. No detrapping is seen during the measurement time which can only be accounted for by deep trapping. Faster trapping and detrapping, causing dispersion, is also visible in the shape of the signal near the transit time around 10 μs. Since our model does not include two trapping constants (shallow and deep), only deep trapping was included in order to reproduce the pulse height. To reproduce the details of the signal rise, some trapping-detrapping with faster time constants would be needed. Apart from the fact that the simulated signal shows a much sharper break at the transit time, compared to the data, the main features of hole transport are well reproduced with a mobility of 15 $cm^2V^{-1}s^{-1}$ and a lifetime of 3.2 μs. This is much smaller than the usually reported hole mobility for CdZnTe. But when using a mobility of 50 $cm^2V^{-1}s^{-1}$ and a lifetime of 5 μs,[12] the collection efficiency of our CdZnTe detector was overestimated.[2] Also the present parameters yield a $\mu\tau$ product of 4.8×10^{-5} cm^2V^{-1} witch is consistent with other measurements where values of a few times 10^{-5} cm^2V^{-1} were reported.[17]

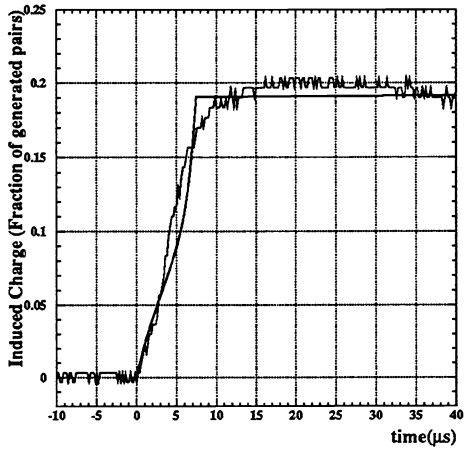

Figure 5. Measured and simulated hole signal induced on a cathode by alphas incident on its center.

Table 1. Transport parameters extracted from the alpha measurements.

	Mobility $cm^2V^{-1}s^{-1}$	Trapping Time	Detrapping Time
Electrons	1000	55 ns	28 ns
Holes	15	3.2 μs	$> 50\mu$s

4. IMAGING

By scanning collimated radiation across contact strips we can measure the pattern of signal sharing among neighboring strips. We performed such scans using both the laser spot and a collimated beam from a ^{57}Co source (122 keV). The results indicate that the relative pulse heights recorded on neighboring strips can be used to measure the event location with a precision significantly finer than the strip pitch.

Figure 6 shows the results of a laser spot scan in 38 μm steps across two cathode pitch lengths. The pulse height for each of the three strips involved (X15, X16, X17) was recorded from its oscilloscope trace for one laser pulse event at each position. The pulse height relative to the sum of the pulse heights from all three strips is plotted. Note that in the gap regions between the contact strips small movements of the laser result in measurable, approximately linear, changes in the relative pulse heights. By contrast, the relative pulse heights remain approximately constant in the regions under the contact strips. Our model's prediction of complete signal collection for events under the contact strip and linear sharing among neighbors for events between strips (see fig. 9) is also shown. These observations indicate that sub-pitch event location capability, perhaps as fine as 10 μm, is possible in the gap regions.

Note also that the flat regions do not extend across the full width of the contact strip. We believe this is due to the space charge effect discussed above. Indeed previous measurements made with a slightly larger and more intense laser beam showed a similar behaviour but with a flat top that was both narrower and lower. Solving the diffusion difficulties encountered with the laser measurements would then make these scan results closer to the model's prediction.

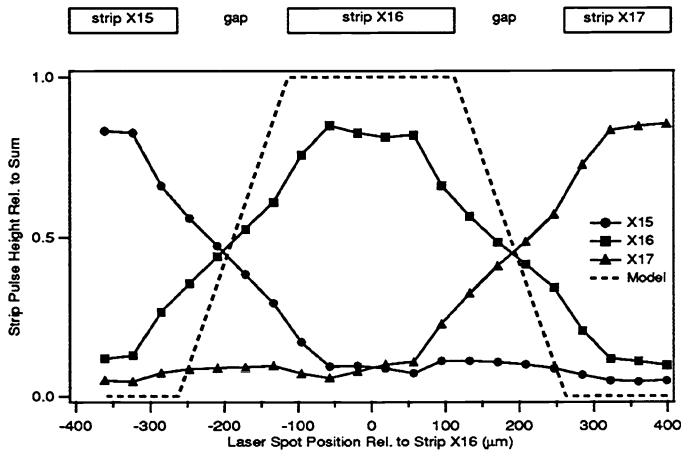

Figure 6. Signal sharing among neighboring strips. Results of a laser spot (40 μm diameter) scan across two cathode pitch lengths.

Concurring results have been obtained with γ-rays. Figure 7 shows histograms of event locations in the x-dimension. Each event position is computed from the strip positions linearly weighted by the relative pulse heights recorded on neighboring strips. These measurements were performed with the prototype strip detector using an 8×8 strip imaging setup and a collimated beam (170 μm diameter) of γ-rays (122 keV) from a ^{57}Co source. The beam spot was scanned over one pitch length (375 μm) over the cathode plane in 75 μm steps, one fifth of a strip pitch. The measurement setup and data acquisition electronics is described in reference.[2] The width of the distribution is mainly due to the collimator diameter. Note that the distribution moves right to left between strips X16 and X15

with each 75 μm step of the collimator but that the difference in the mean position computed by this method is not 75 μm for each step. The largest change in the mean position is observed in the gap region between the contact strips while relatively smaller movement is detected when the gammas interact under the electrode strip. The width of the distribution is also smaller in the strip regions. Note that the weighted average used for computing event locations does not consider the finite width of the contact strips. Figure 8 shows a resolution of about 150 μm in two dimensions which is approximately the collimator diameter. Further studies with better collimated sources will be needed to assess the ultimate imaging resolution of this detector. Sub pitch resolution of less than 50 μm has also been reported for a 100 μm pitch strip detector using 22 keV γ-rays collimated to 30-45 μm on the detector.[6]

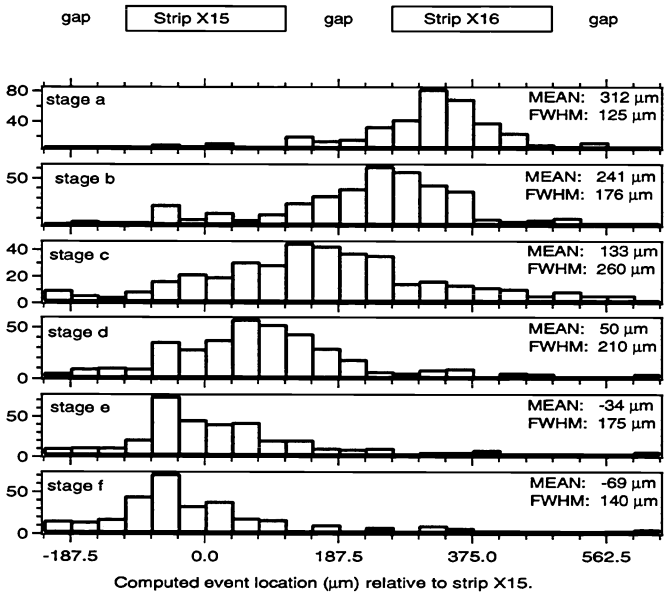

Figure 7. Results of a γ spot (170 μm diameter, 122 keV) scan across one pitch length (375 μm).

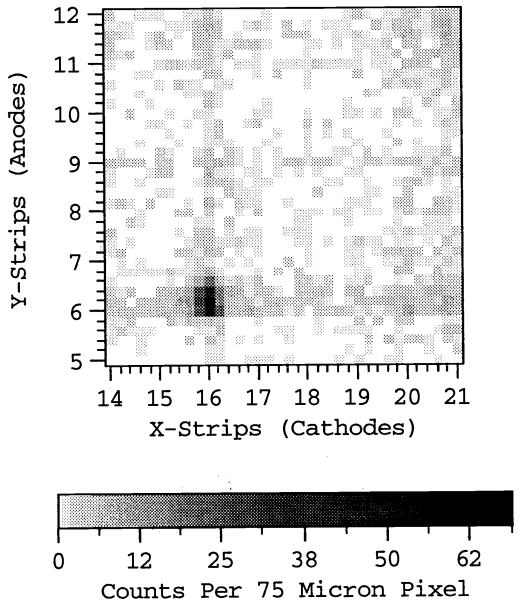

Figure 8. Two dimensional image of gamma spot (122 keV) computed in 75 μm bins.

5. EFFICIENCY

Using the transport parameters extracted from the α-ray signals, the detector response to ^{241}Am and ^{57}Co γ-rays was calculated as a function of the position of interaction in the detector. The modeling process is detailed in reference.[2] A GEANT simulation provides energy deposition spectra as a function of depth for each radioactive source situated at the cathode side. These are folded with the anode and cathode signals calculated by the model over a grid of 375 points in the detector. The simulation includes the transport of both holes and electrons produced in the interaction, the weighting fields of every electrode involved, and the response function of the electronics used during the efficiency measurements. Figure 9 shows relative anode and cathode signal amplitudes of the fast signal outputs used for the trigger. The 15 keV threshold on all anode and cathode channels corresponds to an amplitude of 0.05 for the ^{241}Am photons. A coincidence between the anode and cathode discriminators is required.

With the parameters given in table 1, the calculated efficiency for ^{241}Am is 90% compared with a measured efficiency of 88%. Since those photons are absorbed in a short distance from the cathode, this value is mainly determined by the electron collection efficiency. Such a good agreement is an indication that the limited trapping associated with electrons is quite realistic.

The coincidence detection efficiency (for an absorbed γ-ray) is measured to be 70% for ^{57}Co compared to a calculated value of 95%. In this case, holes play a much more important role in the signal generation. The efficiency variation with the energy is a result of a competition between an increased electron-hole pair generation at higher energy and a decreased charge collection efficiency when higher energy γ-rays interact deeper in the detector. While the experiment indicates that the collection efficiency deteriorates faster than the generated charge increases, the simulation shows the opposite trend. Nevertheless, the agreement is improved compared to simulations made with $\mu_h = 50$ cm^{2}V^{-1}s^{-1} and $\tau_h = 5$ μs.[2] This shows clearly that, though the reduced hole transport properties extracted from the alpha measurements give better efficiency values than before,[2] these are still overestimated. It must be noted that the hole parameters of table 1 have been extracted from a single α-ray signal. These signals exhibit large amplitude fluctuations. Though we attempted to choose a typical event, a slightly lower alpha signal would have resulted in different parameters in table 1 and an improved agreement with the efficiency measurements.

Several avenues will be pursued to resolve the remaining discrepancy. More α signals will be analyzed to obtain an average α response. Laser measurements will be repeated in a more controlled way in order to remove any space charge effect and to allow more precise measurements. New γ-ray response experiments will be made at different energies and with fine collimators and from both detector faces to better measure the detector response as a function of the energy and the position in the detector. Different triggering schemes (by summing a few contiguous channels before discriminating) will also been studied with the aim to define more effective triggers. It is important to obtain a good agreement between such measurements and the model to make realistic predictions of the response of strip detectors of different geometries without the need of actually fabricating too many different prototypes.

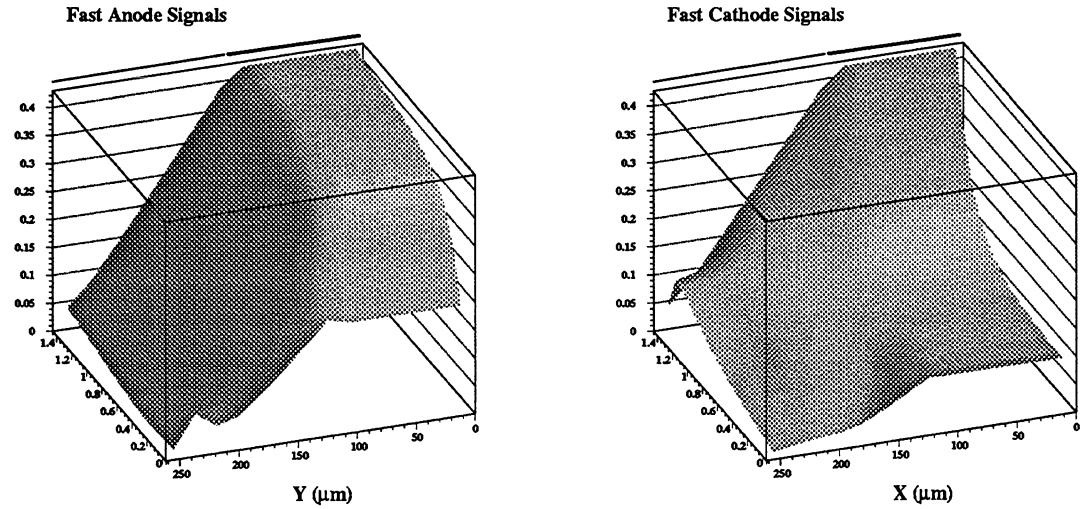

Figure 9. Amplitude of the fast anode and cathode signals.

6. FUTURE WORK

We intend to perform additional simulations and measurements with this strip detector in an effort to gain more confidence that our simulations of the charge transport and signal generation processes sufficiently represent the observed signals. This will require refinement of the pulsed laser system and optics as well as the use of faster preamplifiers. We intend to perform these measurements on other regions of the prototype strip detector and on other prototype devices. Finer gamma collimators or shadow masks will be required for proper measurement of the spatial resolution and point spread function. We will pursue this as well. Also new spectroscopic measurements will be made with these finer collimators to better assess the properties of our detector and to improve our simulation model.

We plan to use the simulation tools developed to predict the performance of strip detectors of different thicknesses having a range of contact strip pitch and strip width. Given the efficiency limitations noted above, different geometries for anodes and cathodes should be considered.

We also plan to consider other imaging electrode configurations in an effort to avoid the efficiency limitations of strip detectors. A brief discussion and some preliminary measurements follow.

While CdZnTe pixel detectors require many more electronic channels than do strip detectors they are excellent imaging spectrometers and, as electron-only sensing devices, they do not suffer from the efficiency limitations described above for strip detectors.[3,9,10] Excellent spectroscopic performance has also been demonstrated with CdZnTe devices employing coplanar anodes.[12,16] Z. He[16] further demonstrates event location capability of these devices in the z, depth, dimension. As these devices rely only on the motion of the relatively mobile electrons for signal generation they are sensitive to interactions occurring over a wider range of distances from the anode plane.

To see if our prototype strip detector would perform as a one-dimensional imager operating in a coplanar anode mode we established different collecting and non-collecting biases on alternate anode strips and collected samples of the signals generated on neighboring strips from the interactions of ^{137}Cs (662 keV) γ-rays. Figure 10 illustrates the test setup and figure 11 is a set of preamplifier output signals from an event triggered by one of the collecting strips.

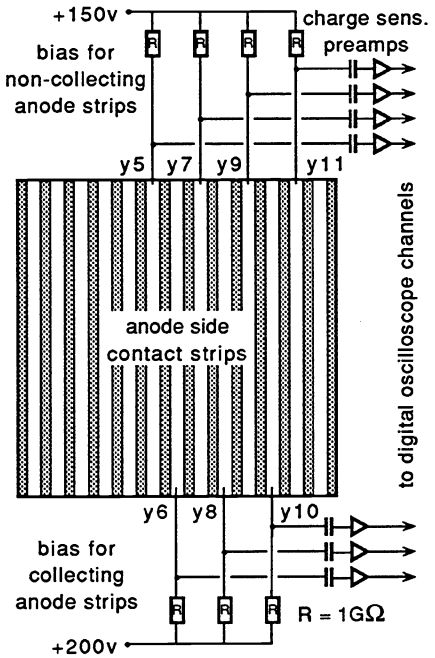

Figure 10. Coplanar anode setup for strip detector test. Signals from seven contiguous anode strips are monitored with digital oscilloscopes. Even numbered anode strips (collecting) are biased at +200 V, odd numbered anode strips are biased at +150 V. Cathode strips (not shown) are biased at ground potential.

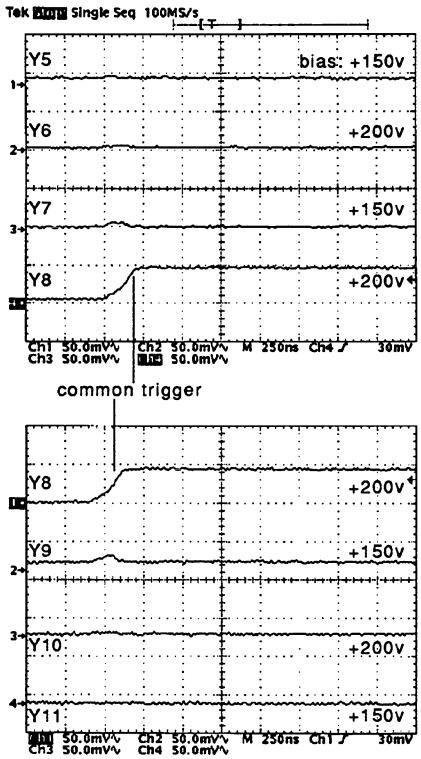

Figure 11. Anode signals from a sample event. Signals from seven contiguous anode strips triggered by the signal on the central collecting strip (Y8). A ^{137}Cs, 662 keV, gamma source was used..

A large sample of events was observed. Figure 11 is a typical event. Note that while the signal is induced on only one collecting strip, a transient signal, with no net charge collected, is observed on each (sometimes just one) of the neighboring non-collecting strips. We observed no events where the signal extended beyond the first neighbor and very few events where there was no signal observed on a neighboring non-collecting strip.

While much more study is required, this observation suggests that strip detectors operated in this mode can serve as one-dimensional imagers with spatial resolution on the order of twice the strip pitch while employing the coplanar grid technique reported by Luke for its spectroscopic advantage. Furthermore, this approach may have efficiency advantages for thicker detectors or when detecting higher energy photons that interact at all depths within the detector. Other anode geometries must be considered in applications requiring imaging in two dimensions. We will pursue these studies.

7. CONCLUSIONS

We have found some encouraging results in our efforts to achieve more quantitative agreement between our CdZnTe strip detector simulations and observations in the laboratory. The scanable focused pulsed laser and the alpha source together with the simultaneous recording of signals from neighboring strips present a powerful tool for the measurement of carrier transport properties. While these measurements require further optimization, particularly with regard to control of the laser pulse, they yielded reasonable values for the transport parameters of our prototype which we then used in our simulation model to predict performance.

The model's predictions of no sharing of signal for interactions under the contact strip and nearly linear sharing of the signal among neighboring strips in the gap region between the strips has been verified both with scans of a laser spot and a gamma beam. These scans reveal that the imaging capability of strip detectors in the gap region is much finer than the strip pitch. By computing event locations linearly weighted by the relative signal recorded on neighboring strips we have clearly observed 38 micron motion of the laser spot and 75 micron motion of the 122 keV

gamma beam. The FWHM measured for the gamma beam distribution is dominated by the 170 micron diameter of the beam spot. A much finer collimator will be required to measure the spatial resolution. These observations suggest that strip detectors can achieve fine spatial resolution with thinner strips on a coarse pitch thus requiring fewer contacts and electronic channels than previously anticipated.

The simulation model confirms the sharp reduction in the cathode collection efficiency observed in the laboratory for interactions which occur far from the cathode surface. This results in reduced efficiency for strip detectors which require coincident anode and cathode triggers. This effect must be considered when designing CdZnTe strip detectors for specific applications. We found agreement between the computed and measured efficiency at 60 keV but additional measurements are required at higher energy and with laser and α-rays to provide more accurate transport parameters, especially for holes.

ACKNOWLEDGEMENTS

We wish to thank J.L. Brebner for his contribution in setting up the laser and the optical system as well as for several useful discussions. We also wish to thank P.F. Hinrichsen for his help with the scanning system and the optics. J. Berichon's work on the mechanical setup is also acknowledged. This work is supported by NASA's High Energy Astrophysics Gamma Ray Astronomy Research and Analysis program and by the Natural Sciences and Engineering Research Council of Canada.

REFERENCES

1. J.M. Ryan et al., "Large Area Sub-Millimeter Resolution CdZnTe Strip Detector for Astronomy", SPIE Conf. Proc. San Diego, **2518**, p. 292, 1995.
2. M. Mayer et al., "Performance and Simulation of CdZnTe Strip Detectors as Sub-millimeter Resolution Imaging Gamma Radiation Spectrometers", to be published in IEEE Trans. Nucl. Sci., 1996 NSS Conference Issue, 1997.
3. H.B. Barber et al., "CdZnTe arrays for nuclear medicine imaging", SPIE Conf. Proc. Denver CO, **2859**, p. 26, 1996.
4. J.R. Macri et al., "Progress in the development of large area sub-millimeter resolution CdZnTe strip detectors", SPIE Conf. Proc. Denver CO, **2859**, p. 29, 1996.
5. J.L. Matteson et al., "CdZnTe strip detectors for high-energy X-ray astronomy", SPIE Conf. Proc. Denver CO, **2859**, p. 58, 1996.
6. P. Kurczynski et al., "CZT strip detectors for imaging and spectroscopy: collimated beam and ASIC readout experiments", in IEEE Nuclear Science Symposium Conference Record, Anaheim CA, p. 671, 1996.
7. L.A. Hamel et al., "Signal Generation in CZT Strip Detectors", IEEE Trans. Nucl. Sci., **43**, p. 1422, 1996.
8. J.A. Heanue, J.K. Brown and B.H. Hasegawa, "Two-dimensional modelling of compound semiconductor strip detectors", in IEEE Nuclear Science Symposium Conference Record, Anaheim CA, p. 548, 1996.
9. J.D. Eskin et al., "The effect of pixel geometry on spatial and spectral resolution in a CdZnTe imaging array", in IEEE Nuclear Science Symposium Conference Record, San Francisco CA, p. 544, 1995.
10. L.A. Hamel and S. Paquet, "Charge transport and signal generation in CdTe pixel detectors", Nucl. Instr. and Meth. A, **280**, p. 238, 1996.
11. L.A. Hamel, "Signal induced in semiconductor detectors with a linear field profile in the presence of trapping and detrapping", submitted to Nucl. Instr. and Meth. A.
12. P.N. Luke, "Unipolar charge sensing with coplanar electrodes Applications to semiconductor detectors", IEEE Trans. Nucl. Sci., **42**, p. 207, 1995.
13. Z. He, "Potential distribution within semiconductor detectors using coplanar electrodes", Nucl. Instr. and Meth. A, **365**, p. 572, 1995.
14. P.M. Morse and H. Feshbach, "Methods of Theoretical Physics", New York: McGraw Hill, chapter 10, 1953.
15. F. P. Doty, "Carrier mobilities and lifetimes in CdTe and CdZnTe", Properties of Narrow Gap Cadmium-based Compounds, P. Capper ed., in Electronic Materials Information Service Data Reviews Series, **10**, p. 540, 1994.
16. Z. He et al., "Position sensitive single carrier CdZnTe detectors", in IEEE Nuclear Science Symposium Conference Record, Anaheim CA, p. 331, 1996.
17. R.B. James, T.E. Schlesinger, J.C Lund and M. Schieber, "$Cd_{1-x}Zn_xTe$ Spectrometers for Gamma and X-Rays Applications" in Semiconductors for Room Temperature Nuclear Detector Applications, T.E. Schlesinger, R.B. James editors, Semiconductors and Semimetals, vol. **43**, Academic Press, San Diego, p. 344, 1995.